

Modeling surface water-groundwater interaction in arid and semi-arid regions with intensive agriculture



Yong Tian, Yi Zheng*, Bin Wu, Xin Wu, Jie Liu, Chunmiao Zheng

Center for Water Research, College of Engineering, Peking University, Beijing 100871, China

ARTICLE INFO

Article history:

Received 10 March 2014

Received in revised form

10 October 2014

Accepted 13 October 2014

Available online

Keywords:

Surface water-groundwater interaction

Integrated modeling

GSFLOW

SWMM

Heihe River Basin

ABSTRACT

In semi-arid and arid areas with intensive agriculture, surface water-groundwater (SW-GW) interaction and agricultural water use are two critical and closely interrelated hydrological processes. However, the impact of agricultural water use on the hydrologic cycle has been rarely explored by integrated SW-GW modeling, especially in large basins. This study coupled the Storm Water Management Model (SWMM), which is able to simulate highly engineered flow systems, with the Coupled Ground-Water and Surface-Water Flow Model (GSFLOW). The new model was applied to study the hydrologic cycle of the Zhangye Basin, northwest China, a typical arid to semi-arid area with significant irrigation. After the successful calibration, the model produced a holistic view of the hydrological cycle impact by the agricultural water use, and generated insights into the spatial and temporal patterns of the SW-GW interaction in the study area. Different water resources management scenarios were also evaluated via the modeling. The results showed that if the irrigation demand continuous to increase, the current management strategy would lead to acceleration of the groundwater depletion, and therefore introduce ecological problems to this basin. Overall, this study demonstrated the applicability of the new model and its value to the water resources management in arid and semi-arid areas.

© 2014 Elsevier Ltd. All rights reserved.

Software availability

Name: GSFLOW-SWMM

Program language: Fortran and C

Developers: Dr. Yong Tian (yongtian@pku.edu.cn) and Dr. Yi Zheng (yizheng@pku.edu.cn), Center for Water Research, College of Engineering, Peking University, Beijing 100871, China

Availability: Contact the developers

1. Introduction

In arid and semi-arid regions, interaction between surface water (SW) and groundwater (GW) plays an important role in the eco-hydrological system (Sophocleous, 2002; Gilfedder et al., 2012). The interaction is often complicated by agricultural activities including surface water diversion, groundwater pumping and irrigation, as they could significantly alter the flow regimes of both surface water and groundwater (Barlow et al., 2000; McCallum et al., 2013; Shah, 2014; Siebert et al., 2010). Understanding the complex behavior of the integrated SW-GW system is very

important to the regional water resources management (Rassam et al., 2013), and integrated modeling is a highly desired approach.

A number of integrated SW-GW models have been developed, such as GSFLOW (Markstrom et al., 2008), HydroGeoSphere (Brunner and Simmons, 2012; Therrien et al., 2010), ParFlow (VanderKwaak and Loague, 2001), MIKE SHE (Graham and Butts, 2005), MODHMS (Panday and Huyakorn, 2004) and SWATMOD (Sophocleous et al., 1999). Some of these models incorporate MODFLOW (Harbaugh, 2005), a classic 3-D groundwater simulator, as their subsurface module. For example, GSFLOW integrates Precipitation Runoff Modeling System (PRMS) (Leavesley et al., 1983) with MODFLOW; SWATMOD couples the widely applied Soil Water Assessment Tool (SWAT) (Arnold et al., 1998) model with MODFLOW; and MODHMS introduces 2-D diffusion wave routing for surface water into MODFLOW. The existing models have been applied to address different water resources issues, including irrigation management (e.g., Pérez et al., 2011), SW-GW interactions (e.g., Huntington and Niswonger, 2012; Niswonger et al., 2008; Werner et al., 2006), land use and climate change (e.g., Graham and Butts, 2005; Markstrom, 2012), water quality (e.g., Borah and Bera, 2003) and so on.

However, few studies (Demetriou and Punthakey, 1998) have investigated the hydrologic impacts of agricultural water use in the context of integrated SW-GW modeling, especially for large river

* Corresponding author.

E-mail address: yizheng@pku.edu.cn (Y. Zheng).

basins. The lack of research is in part due to the limited capacity of the existing integrated models in simulating the complicated flow regime in an irrigation system. For example, unlike a natural river network in which tributaries run into the main stream, an irrigation network has a main aqueduct which splits water into lower-order aqueducts. Also, engineering structures (e.g., culverts, weirs, gates, and pumps) and their operations in irrigation systems are often ignored by the existing models. Hydraulic modules in the current models are not able to handle these complexities. On the other hand, some studies (Rassam, 2011; Rodriguez et al., 2008; Valerio et al., 2010; Welsh et al., 2013) introduced advanced hydraulic engines (e.g., HEC-RAS, RiverWare, SIMS) into MODFLOW, but the basin-scale SW-GW interaction was not fully accounted for.

To better address the role of agricultural water use in integrating SW-GW modeling, this study coupled GSFLOW with SWMM (Rossman, 2009). To our best knowledge, this coupling has not been attempted by previous studies. SWMM is a dynamic and distributed model for simulating runoff quantity and quality. It has been widely used to study different rainfall-runoff issues (Gironás et al., 2010; Peterson and Wicks, 2006; Shrestha et al., 2013). Its hydraulic engine can nicely handle the flow in artificial waterways with different engineering structures. GSFLOW's strength in modeling SW-GW interaction and SWMM's strength in hydraulic simulation complement each other. In addition to the coupling, two modules were added, one to allocate diverted water from aqueducts to farms, and the other to allocate pumped water from wells to farms.

The coupled model (hereafter called GSFLOW-SWMM) was then applied to Zhangye Basin (ZB), a typical arid and semi-arid area in northwest China. ZB is the mid-stream part of Heihe River Basin (HRB), which is the second largest inland river basin in China. The SW-GW interaction in ZB is significant and complicated (Hu et al., 2007), and highly impacted by agricultural irrigation which consumes a great amount of water from the Heihe River and local aquifers. Securing the environmental flow towards the downstream has been an important management issue, due to the fast degradation of the ecosystem in the lower HRB (the Gobi Desert area) and the shrink of the terminal lake, the Juyan Lake (Guo et al., 2009). Hydrological modeling has been performed for both the entire HRB and ZB alone (Li et al., 2013, 2010; Wang et al., 2010; Wen et al., 2007; Zhang et al., 2004), but fully integrated SW-GW modeling has not been attempted for this area.

Overall, this study was aimed to: 1) enhance the capability of the integrated SW-GW modeling in addressing highly engineered flow systems such as the agricultural irrigation system; and 2) demonstrate how the integrated modeling would benefit the hydrological process understanding and water resources management at large basins. In the remaining of this paper, Section 2 introduces the coupling strategy and additional modules added. Section 3 describes the study area and the modeling procedure. Results and discussion are presented in Sections 4, and conclusions are provided in Section 5.

2. Modeling framework

2.1. Introduction to GSFLOW and SWMM

GSFLOW (Coupled Ground-Water and Surface-Water Flow Model) is a model developed by USGS (Markstrom et al., 2008) which simulates all major processes of the hydrologic cycle. It integrates PRMS with MODFLOW which perform surface hydrology simulation and 3-D groundwater simulation, respectively. The MODFLOW2005 version adopts the UZF package (Niswonger et al., 2006) as its unsaturated-zone flow simulation module, the SFR2 package (Niswonger and Prudic, 2005) as its streamflow module, and the WELL package to account for groundwater pumping. In the

PRMS domain, GSFLOW delineates the study area into hydrologic response units (HRUs), with the aid of external tools such as ArcSWAT. HRUs can be grouped into sub-basins, and each sub-basin contains one “river segment”. The delineation of the subsurface domain follows the standard procedure of MODFLOW. The portion of the river segment within a MODFLOW grid is referred to as a “reach”. A river segment usually consists of multiple reaches. GSFLOW generally runs at a daily time step, but its SFR2 component can take sub-daily time steps (e.g., hourly). GSFLOW defines “gravity reservoir” as a storage in which an HRU exchanges water with the MODFLOW grid(s) it intersects. In reaches where stream water is connected with groundwater, the stream-aquifer exchange is calculated based on the head difference using Darcy's law. More details about GSFLOW can be found in Markstrom et al. (2008).

SWMM conceptualizes four compartments including atmosphere, land surface, groundwater and transport (i.e. drainage network). In the model, precipitation is transferred from atmosphere to land surface, and then either is delivered as runoff to the transport compartment or infiltrates into groundwater. The groundwater compartment is segmented into upper unsaturated zone and lower saturated zone. Water fluxes leaving the two zones including evapotranspiration (ET), lateral interflow to the transport compartment, and percolation to deep groundwater, which are calculated by the model. A simple mass balance calculation is applied to determine the storage change. SWMM uses a node-link scheme to represent a drainage network. A link controls the rate of flow from one node to another. Links are typically conduits (open channels and pipes), but can also be orifices, weirs or pumps. A node accepts runoff from the sub-catchment it links. Tributary flows, inflows or diversions could also be specified for nodes. There are four types of nodes in SWMM, junction, divider, outfall and storage unit. A junction is a connection where links join together. Dividers are drainage system nodes that divert inflows to a specific conduit in a prescribed manner. Outfalls are terminal nodes of the drainage network used to define downstream boundaries. Storage units provide water storage capacities at specific locations.

SWMM has an advanced hydraulic simulation engine, which is able to handle large-size drainage networks and simulate complicated flow regimes (e.g., backwater, reverse flow, etc.). It can also simulate various hydraulic structures and their operations. The engine employs finite difference method to solve one-dimensional Saint-Venant equations, either using kinematic wave (KW) method or dynamic wave (DW) method. The time and spatial resolutions for the hydraulic calculation vary, and could be determined based on the courant condition. SWMM allows stand-alone hydraulic simulations if input hydrographs are provided, and therefore it is practical to embed its hydraulic engine into other models, as attempted by this study.

Although GSFLOW and SWMM both simulate a complete hydrologic cycle, they are different in many aspects (see Table 1). The major difference relevant to the integrated SW-GW modeling for agricultural areas including the following. First, the node-link structure in SWMM offers greater flexibility in representing complicated drainage networks with different hydraulic structures. In GSFLOW, inflows are only allowed for the first (i.e., upmost) reach of a river segment. Water diversion is only allowed for the last (i.e., lowermost) reach of a segment, and its magnitude has to be constant within one stress period. In addition, GSFLOW does not consider hydraulic structures and their operations. The second major difference lies in flow routing. The SFR2 module in GSFLOW only uses KW method, while SWMM can also solve the full Saint-Venant equations with the DW method. Although more computationally expensive, the DW method would provide more accurate results than the KW method (Singh, 2001; Vieira, 1983), especially for complicated flow regimes. The third major difference

Table 1
Comparison between GSFLOW and SWMM.

Aspects	Functionality	Model	
		GSFLOW	SWMM
Hydraulics	Flow routing	Mass conservation or kinematic wave	Kinematic wave or dynamic wave
	Numerical method for flow routing	Implicit finite difference method	Explicit finite difference method
	Flow regimes	Steady-uniform flow and unsteady flow	Steady-uniform flow, unsteady flow, backwater and reverse flow
	Simulation of hydraulic structures	No	Yes (e.g., dividers, pumps, weirs, orifices, etc.)
	Dynamic control rules	Only allowed for diversion of specified flow at the last reach of a river segment	Allowed. The model enables to apply user-defined control rules for the operation of various hydraulic structures
Hydrology	Surface runoff and Infiltration	Uses a linear or nonlinear variable-source-area method with cascading flow allowed	Uses a nonlinear reservoir model to simulate surface runoff and provides three options to simulate infiltration
	Unsaturated-zone flow	Adopts kinematic-wave approximation to Richards' equation	Not explicitly considered
Water quality	Groundwater flow	3D finite-difference model	Mass balance model
	Pollutants modeled	No	Yes
	Treatments	No	Yes

is related to SW-GW exchange. In SWMM, the calculation of groundwater head and SW-GW exchange is highly simplified, and the flow in the unsaturated zone is not explicitly considered. In GSFLOW, the exchanges are sophisticatedly modeled with the following strategies.

- 1) *HRU-grid exchange*. GSFLOW conceptualizes a gravity reservoir in soil, which contains the soil water above field capacity that is not subject to preferential flow. Water in the gravity reservoir may leak into unsaturated zone (or vadose zone), a layer between the soil layer in PRMS and the shallow aquifer in MODFLOW. The water moving out of the bottom of unsaturated zone becomes the recharge to the shallow aquifer. The unsaturated-zone flow is simulated by the UZF package (Niswonger et al., 2006). The gravity reservoir also accepts groundwater discharge whenever the groundwater head calculated by MODFLOW exceeds the top of unsaturated zone. Furthermore, if the groundwater head is above land surface, the groundwater turns into overland flow which could be routed to adjacent rivers or lakes.
- 2) *Stream-aquifer exchange*. In GSFLOW, three types of stream-aquifer interaction are considered: gaining (direct exchange from aquifer to stream), losing (direct exchange from stream to aquifer) and disconnected (no direct exchange). In both gaining and losing situations, the groundwater head exceeds the bottom of streambed, and the exchange flux is calculated based on the difference between the head and stream stage using the Darcy's law. In the disconnected situation, the water in stream leaks out of the streambed into the unsaturated zone beneath it, and moves towards the shallow aquifer. In this case, the water flux into the unsaturated zone is calculated based on the Darcy's law, considering the head difference between the stream stage and the bottom of streambed. The stream-aquifer interaction is handled by the SFR2 package (Niswonger and Prudic, 2005).

It is clear that GSFLOW and SWMM (specifically its hydraulic simulation engine) can complement each other in modeling the SW-GW interaction impacted by agricultural water use. This important observation motivated our model coupling study.

2.2. Coupling of the models

The coupling of GSFLOW (version 1.6.1) and SWMM (version 5.0) was implemented using Microsoft Visual Studio 2010 and Intel Visual FORTRAN Compilers 11 for Windows. Since the programming languages are FORTRAN and C for GSFLOW and SWMM,

respectively, significant efforts were made to reconcile C functions with FORTRAN subroutines. Three major issues need to be appropriately addressed in the coupling. The first one is to enable the two-way water exchange between links in SWMM and subsurface grids in GSFLOW. The second one is to allow user-specified diversion rates in the model. The third one is to adapt the time scale of stream-aquifer exchange calculation to the time scale of the DW routing in SWMM. To resolve these issues, following modifications or developments have been made.

Fig. 1 illustrates a typical SWMM drainage network embedded in the GSFLOW domain. In GSFLOW-SWMM, junctions are defined at the locations where the drainage network intersects the edges of subsurface grids, as well as at those confluent points. Other types of nodes are similarly defined as in the original SWMM. Overland flow and interflow from HRUs, simulated by GSFLOW, are transfer to adjacent nodes. According to the scheme in Fig. 1, a conduit between two nodes is located in a single grid, while one grid may contain multiple conduits.

In GSFLOW-SWMM, the hydraulic engine of SWMM replaces SFR2 in simulating the flow in the drainage network. Nevertheless, to compute the SW-GW exchange between each conduit and its associated subsurface grid, the algorithm in SFR2, as introduced in Section 2.1, was kept and re-coded into the hydraulic engine of SWMM. Conduits in SWMM do not have the properties in relation to stream-aquifer interaction, such as thickness and vertical hydraulic conductivity of streambed. These properties were added onto the conduits in GSFLOW-SWMM. The water head of a conduit is computed as the average head of the nodes it links. Also, SWMM was modified to allow direct precipitation into and evaporation from a conduit.

SWMM can flexibly represent water diversion from conduits using four types of dividers (cutoff, overflow, weir and tabular dividers). However, users can only specify diversion rules. For example, at a weir, the diversion rate is automatically determined by a prescribed weir equation. SWMM does not handle user-specified diversion rates at dividers. Thus, a new type of divider, named as "schedule divider", was added in GSFLOW-SWMM which accepts user-defined time series of diversion rates. Diversion is operated following the pre-defined rates, unless the rate in a calculation step exceeds the available flow, in which case all the available flow is diverted.

In GSFLOW, the time steps for the KW routing and stream-aquifer exchange calculation are kept the same. The DW routing in SWMM requires a much finer time step (usually less than 1 min) than the exchange calculation (usually an hour). The computational cost of a model run would be very high if the time step for the DW

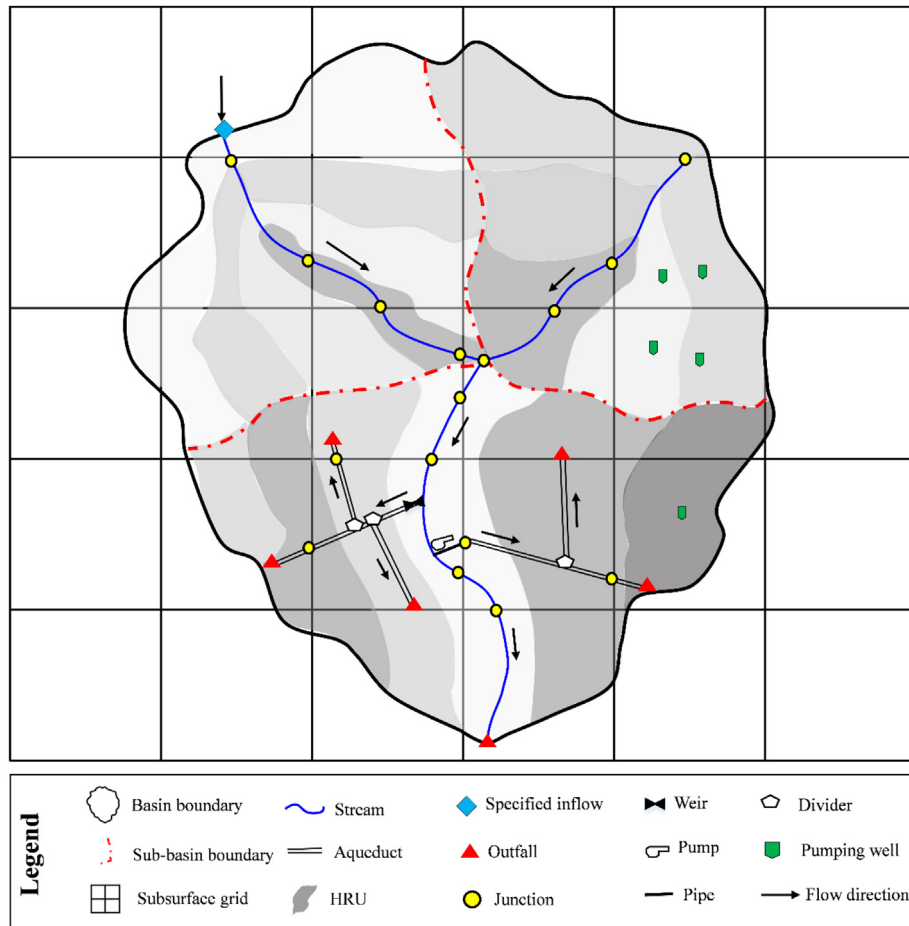


Fig. 1. Schematic representation of a typical SWMM drainage network in the GSFLOW domain.

routing is applied to the exchange calculation. To reduce the cost, GSFLOW-SWMM allows to assign different time steps for the DW routing and the exchange calculation.

2.3. Additional modules

Irrigation is rarely explicitly considered in integrated SW-GW modeling at a large basin scale. Irrigation practice mainly consists of water withdrawal from sources (e.g., rivers, lakes, and wells), water conveyance, and distribution of water in the field. SWMM can easily deal with the water withdrawal process as its divider and pumping node objects can represent different intake structures. The conveyance system can be simulated in terms of conduit objects (e.g., rivers and aqueducts) and regulator objects (e.g., pumps, gates and weirs) in SWMM. However, the water distribution process has not been addressed by either SWMM or GSFLOW. In GSFLOW-SWMM, a module was added to transfer surface water from a divider or outfall to its linked HRUs. Another module was similarly developed to transfer groundwater from each pumping well to HRUs it connects. Only the HRUs with farm lands are irrigated. In both modules, the water from a conduit or a well is allocated among its linked farm land HRUs in proportion to the area fractions of the targeted HRUs. The water allocated to each HRU is then treated as “pseudo rainfall”, and combined with the original rainfall to the HRU in the following model calculation.

Evapotranspiration (ET) is a critical concern in arid and semi-arid areas with intensive agriculture. GSFLOW provides two options for computing potential ET (PET): Hamon formulation and

Jensen-Haise formulation. These two empirical methods can be easily applied in data-limited cases, but have many limitations (Adeboye et al., 2009; Markstrom, 2012). To improve the ET calculation, we coded the FAO Penman-Monteith (FAO-PM) method (Allen et al., 1998) in GSFLOW-SWMM as an additional option. If adequate meteorological data are available, FAO-PM appears to be a more reliable method (Fisher et al., 2011).

3. Case study

3.1. Study area

Our study area (Fig. 2), the Zhangye Basin (ZB), is the midstream region of Heihe River Basin (HRB). It is a sedimentary basin bounded by the Qilian Mountains on the south, the Bei Mountains on the north, the Jiuquan-west Basin on the west and the Maying Basin on the east. Yingluoxia and Zhengyixia are the starting points of the midstream and downstream of the Heihe River, respectively. The modeling domain has an area of 9097 km², and the elevation ranges from 1290 m in the northwest to 2200 m in the southeast. The landscape is featured by irrigated farmlands in oasis surrounded by desert with very poor vegetation. As of 2000, the irrigated farmlands account for 26.9% of the total area. Corn and winter-wheat are the main crops. A complicated aqueduct system has been built in this area. The rest of the area consists of forests (1.4%), grassland (14.5%), urban areas (2.4%), water bodies (2.7%), and vacant lands (52.2%).

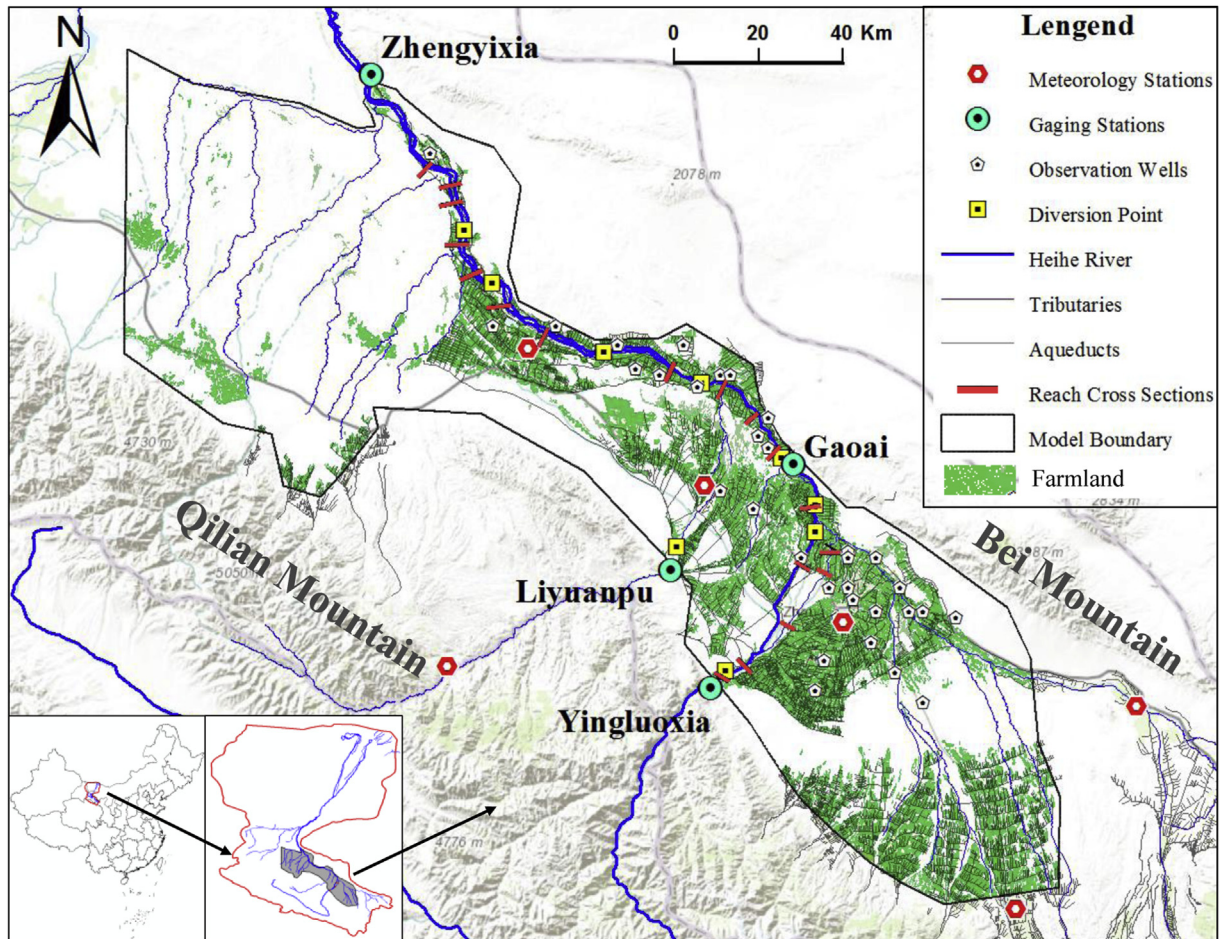


Fig. 2. The study area and modeling domain.

The average annual rainfall in ZB is about 190 mm, mainly in June to September. The average annual PET was estimated to be 1325 mm (Wu et al., 2010). According to the flow monitoring data between 2000 and 2008, on average 2.22 billion m^3/year of surface water enters this area from the Qilian Mountains (as rainfall runoff and snowmelt water), and 1.72 billion m^3/year is through Yingluoxia. The local precipitation mainly converts to ET and infiltration water, producing limited surface runoff. The surface outflow is mainly through Zhengyixia and is 0.97 billion m^3/year (2000–2008) on average. According to 2000–2008 statistics from the local water resources authority, the agriculture takes about 2.08 billion m^3/year , 83% of which is surface water diverted from the Heihe River, and the rest is pumped groundwater. The intensive agricultural water use in ZB has led to depletion of renewable groundwater and drying of the terminal lake. As the groundwater plays a critical role in sustaining the vulnerable eco-system, its depletion would cause severe environmental and ecological problems, such as decay of springs and wetlands, deterioration of water quality, exacerbation of soil salinization, and degradation of vegetation (Feng and Cheng, 2001; Luo et al., 2005; Liu et al., 2010).

Due to the hydrogeological conditions, the SW-GW interaction in this area is significant and complicated. The groundwater is mainly recharged by stream leakage over the alluvium fans near Yingluoxia, and discharges near the edge of the fans as spring flows or directly from lower riverbeds (Chen et al., 2006). The interaction is strongly impacted by agricultural activities. Water diversion would significantly alter the river water level, and therefore affect

the water exchange across the streambed. Seepage from aqueducts, and irrigation return flow may also recharge the local aquifers.

3.2. Data collection and model setup

Data used in this modeling were acquired from the Cold and Arid Regions Science Data Center (<http://westdc.westgis.ac.cn>) operated by Cold and Arid Regions Environmental and Engineering Research Institute, Chinese Academy of Science, unless otherwise explained. The geospatial datasets used to setup the GSFLOW-SWMM model include Digital Elevation Model (DEM) of 90 m-resolution, digital maps of the land cover in 2000 (1:100,000 scale) and soil types (1:1,000,000 scale). DEM, land cover and soil type data were used to define and parameterize HRUs. DEM data were also used to determine the top elevation of MODFLOW grids and streambed. The hydrogeological information of the study area was collected from the literature (Cheng et al., 2009; Hu et al., 2007; Wen et al., 2007; Wu et al., 2010; Zhang et al., 2004), based on which the subsurface layers were defined and MODFLOW was initially parameterized. The digitized drainage network (including streams and aqueducts) was also achieved, along with the geometric information on the 21 cross sections of the main stream (Fig. 2).

Daily meteorological data including precipitation, temperature (maximum, minimum and average), air pressure, relative humidity, wind speed and direction, and sunshine hour were the major model inputs. The meteorological data (2000–2008) at six weather

stations (see Fig. 2) were collected and extrapolated to each HRU using the Gradient plus Inverse Distance Weighting (GIDW) method (Nalder and Wein, 1998).

River diversion and groundwater pumping data are also important model inputs. The monthly diversion and yearly pumping data of the 20 irrigation districts in this area were collected from the local water resources authority of the Zhangye City. For some of the districts, we only obtained yearly diversion data, and their monthly estimates were determined on the basis of intra-month allocation pattern observed from other districts. In order to improve simulations of daily streamflow, daily diversion data were estimated by downscaling the monthly data based on our investigation on the local agricultural practice and analysis on the observed hydrographs of the Heihe River. For each individual district, the daily estimates may not be accurate, but for the study area as a whole they reflect well the intra-month variation of the diversion. Pumping was taken into account with the Well module of GSFLOW. As we only have yearly pumping data by districts, a constant pumping rate was applied uniformly in each district in each year. The rate only varies across years and across districts.

The modeling domain is similar to that in Hu et al. (2007). The south and north subsurface boundaries used specific flow conditions, receiving groundwater flow from the Qilian Mountains and the Bei Mountains, respectively. The boundary flow fluxes were initially estimated based on the observed hydraulic gradient of the groundwater and the hydraulic conductivity near the boundary (Wu et al., 2010). No-flow conditions were applied to the west and east subsurface boundaries, since there exist groundwater divides (Hu et al., 2007). The daily flow rates at the Yingluoxia and Liyuanpu stations were used as surface water boundary conditions.

The surface domain was delineated into 104 sub-basins and 588 HRUs. The subsurface was divided into five layers, each with 9106 active cells (1 km × 1 km). The first layer represents an unconfined aquifer, the second and fourth layers represent aquitards, and the third and fifth layers represent confined aquifers. From the top to the bottom, the five layers were respectively divided into 21, 12, 14, 12, and 14 zones for model parameterization. The drainage network in the model is comprised of 1697 junctions, 18 outfalls, 12 schedule dividers (i.e., the 12 diversion points shown in Fig. 2) and 1594 conduits (i.e., river and aqueduct elements). As we only have the cross-section details for the main stream, rectangular cross sections were assumed for conduits not in the main stream. The streambed hydraulic conductivity and Manning's roughness coefficient were estimated based on field surveys and the hydrogeological information we collected. With all the necessary data collected, the model was setup with external tools including ArcGIS and ModelMuse.

Note that, besides streamflow and groundwater level, GSFLOW outputs a number of state variables (e.g., soil moisture, canopy storage, stream storage, saturated zone storage, etc.) and fluxes (e.g., ET, surface water infiltration, groundwater exfiltration, stream leakage, interflow, etc.). Thus, a detailed regional water budget, as well as the flux between the budget items, can be readily achieved with the model simulation. Conceptually, for the study area, the major water inputs, with descending importance, are upstream surface inflow, local precipitation and lateral groundwater inflow from the south (Qilian Mountains) and north (Bei Mountains) boundaries. The major water outputs are ET and surface water outflow (mostly through Zhengyixia), and no lateral groundwater outflow has been assumed. Internal water exchanges mainly include surface water recharge to unsaturated zone and saturated zone, and groundwater discharge to land surface and stream. Nevertheless, a coherent and quantitative understanding of the regional water budget is yet to be developed. This study applied the coupled GSFLOW-SWMM model to achieve this.

3.3. Model calibration

Daily streamflow observations (2000–2008) were obtained at four gaging stations (Fig. 2). Observations at the Yingluoxia and Liyuanpu stations were used to set the surface water boundary conditions, and observations at the Gaoai and Zhengyixia stations were used for the model calibration. Monthly groundwater level measurements (2000–2004) at 35 observation wells (see Fig. 2) were obtained and used for the calibration as well.

To set the initial condition for transient simulations, a steady-state MODFLOW simulation was first performed, which is a common practice in applying MODFLOW. Key groundwater parameters (i.e., hydraulic conductivities) were adjusted in this stage. In the next stage, the GSFLOW-SWMM model was run at a daily time-step for a nine-year period from 01/01/2000 to 12/31/2008 (the time-step for the SW-GW exchange calculation is hourly). To have a reasonable initial storage of the soil zone (Huntington and Niswonger, 2012), the first year was treated as a “spin-up” period and therefore excluded from the calibration. Key model parameters for both surface water and groundwater were further tuned to reproduce the observed temporal variability of streamflow and groundwater level. Additional information was referred to further constrain the model calibration, including the ET information drawn from remote sensing data (Li et al., 2012), the regional SW-GW exchange and groundwater storage change estimated by water balance calculation (Cheng et al., 2009), as well as river bed leakage estimated from field measurements and isotope experiments (Wu et al., 2010).

The calibration was manually accomplished in a trial-and-error manner. For groundwater level, after the hydraulic conductivities were adjusted through steady-state simulations, specific yields were further tuned through transient simulations. As we do not have temporally and spatially detailed information on the local pumping which would significantly alter the groundwater level, the calibration was aimed to capture the long-term characteristics of the regional groundwater level, rather than to precisely reproduce the dynamics of groundwater level in individual wells. For streamflow, besides the classic Nash-Sutcliffe model efficiency (NSE) (Nash and Sutcliffe, 1970), two additional goodness-of-fit measures, logNSE and percentage bias (BIAS), were considered. Compared to NSE, logNSE is less sensitive to peak flow. BIAS measures whether the flow is systematically overestimated (positive BIAS) or underestimated (negative BIAS). A limited number of parameters were found to be critical to streamflow calibration. The major adjusted ones include soil's maximum available capillary water-holding capacity, maximum depth where evapotranspiration can occur and maximum possible area contributing to surface runoff in PRMS, and hydraulic conductivity of streambed in the modified hydraulic engine of SWMM. Note that specific yield and horizontal hydraulic conductivity were also found to be important to the streamflow calibration, but they were mainly tuned in the groundwater calibration.

In addition, our preliminary tests showed that using the dynamic wave (DW) method for flow routing (with a time-step of 30 s) instead of the kinematic wave (KW) method made no significant differences in this modeling case. Therefore, the KW method was used throughout this study to save the computational cost.

3.4. Sensitivity analysis

To further explore how major model outputs respond to major input variables, a simple one-factor-at-a-time (OAT) sensitivity analysis (SA) was performed. Thirteen model outputs were considered, including ET, soil moisture (SM), infiltration (IFL), UZF

recharge (UR) (i.e., the recharge from HRU to shallow aquifer), surface leakage (GE) (i.e., groundwater exfiltration to land surface), stream leakage (R2G), groundwater discharge to stream (G2R), surface water to groundwater (S2G) (i.e., sum of R2G and UR), groundwater to surface water (G2S) (i.e., sum of G2R and GE), groundwater level (H), streamflow at the outlet (R), change of total water storage (ΔS_{total}) and change of saturated zone storage (ΔS_{gw}). ΔS_{total} is the sum of the storage changes in four compartments including surface, soil zone, unsaturated zone and saturated zone. The surface storage can be further decomposed into plant canopy, snowpack, impervious surface and stream storages.

Based on our understandings of the water cycle in this area and the manual calibration processes, nine input variables were selected for the SA, as summarized in Table 2. Precipitation (PCP) is an important input data that drive the model simulation, and GW lateral inflow (GWB) represents a critical boundary condition. Both PCP and GWB involve significant data error or uncertainty, which is why they were included. The other seven are all key model parameters as revealed in the manual calibration. In the SA, the input variables, one at a time, were varied from its initial or calibrated values by $\pm 20\%$, and the elasticity of the model outputs (i.e., the percentage change of a model output divided by the percentage change of an input variable) with respect to the $\pm 20\%$ changes was considered as the sensitivity indicator. Note that all the input variables except maximum possible area contributing to surface runoff (CAM) are either dynamic or spatially distributed, and the $\pm 20\%$ changes were uniformly (in time or space) applied to the input variables.

3.5. Scenario analysis

Before 2000, the surface water diversion for irrigation was poorly regulated in ZB, although the State Council had approved a plan for surface water allocation between ZB and the lower HRB. The luxurious agricultural water use in ZB had caused fast degradation of the ecosystem in the Gobi desert and shrink of the Juyan Lake. To protect the unique but fragile eco-hydrological system of the lower HRB, the allocation plan has been strictly enforced since 2000. The plan specifies the amounts of environmental flow (from ZB to the lower HRB) to be secured under different hydrological conditions. For example, in a normal year (i.e., the annual flow from Yingluoxia reaches 15.8 billion m^3), the flow from Zhengyixia towards the downstream should be no less than 9.5 billion m^3 . The regulation has resulted in more surface water available to the lower HRB, and the ecosystem appears to be recovering. However, the decreased water diversion has led to a significant increase of groundwater pumping in ZB. The pumping practice has been largely unregulated, and the problem of groundwater over-exploitation is looming in certain parts of this area.

In this study, the calibrated GSFLOW-SWMM model was applied to examine the potential impact of different water-use scenarios on

Table 3

Simulated management scenarios (S0 is the baseline scenario).

Scenario ID	Irrigation water from diversion (billion m^3)	Irrigation water from pumping (billion m^3)	Total irrigation water (billion m^3)	Percentage of SW replaced by GW
S2	1.901	0.178	2.079	-10%
S1	1.814	0.265	2.079	-5%
S0	1.728	0.351	2.079	0
S3	1.642	0.437	2.079	+5%
S4	1.555	0.524	2.079	+10%

the hydrologic cycle in ZB, as well as the management implications of the impact. Table 3 summarizes the five scenarios compared in this study. S0 is the baseline scenario which represents the actual conditions of the model calibration period (2001–2008). S1 and S2 are two scenarios in which the baseline surface water diversion is increased by 5% and 10%, respectively, compared to S0, while the total irrigation water is kept unchanged. Similarly, S3 and S4 are two scenarios in which 5% and 10% of the baseline diversion is respectively replaced by the same amounts of pumped groundwater. Note that in this scenario analysis these percentage changes were uniformly applied in time and space. As the total amount of water for irrigation is the same in the five scenarios, the comparison would reveal the effect of the substitution between surface water and groundwater for the irrigation in ZB.

4. Results and discussion

4.1. Calibration results

Fig. 3 compares the monthly streamflow simulated by GSFLOW-SWMM against the observations at the Gaoai and Zhengyixia stations. The Nash-Sutcliffe model efficiency (NSE) is 0.885 at the Gaoai station and 0.884 at the Zhengyixia station. The logNSE equals to 0.837 and 0.602, and the BIAS equals to 0.09 and -0.04 for the two stations, respectively. For daily streamflow (not illustrated), the NSE equals to 0.833 and 0.831, respectively. These goodness-of-fit metrics indicate that, the model adequately reproduced the observed hydrographs overall, especially at the monthly time scale. Fig. 4 compares the observed and simulated average groundwater levels (for the period 2001–2004) at the 35 monitoring wells (refer to Fig. 2). All the circles are close to the 45-degree line, and the deviation from the line is less than 2.5 m for over 60% of the circles. Overall, the model well captures the long-term characteristics of the regional groundwater level. It is worth re-emphasizing that, in this case study, the calibration was not aimed to precisely reproduce the daily-scale or monthly-scale dynamics of groundwater level for individual wells, since the dynamics may be substantially impacted by the local pumping rates on which we do not have temporally and spatially detailed information. Nevertheless, for

Table 2

Input variables considered in the sensitivity analysis.

Model parameter or input	ID	Main process(es) represented	Calibrated value ^a
Precipitation (mm/day)	PCP	Driving force	/
GW lateral inflow (m^3/year)	GWB	Boundary condition	/
Horizontal hydraulic conductivity (m/day)	HK	GW flow	0.15–120
Vertical hydraulic conductivity (m/day)	VK	GW flow and infiltration	0.015–12
Hydraulic conductivity of streambed (m/day)	RVK	River bed leakage	0.05–1.1
Specific yield (dimensionless)	SY	GW flow	0.15–0.3
Soil's maximum available capillary water-holding capacity (cm)	SMM	ET, infiltration and surface runoff	14–33
Maximum depth where evapotranspiration can occur (cm)	SRM	ET and infiltration	10.2–24.4
Maximum possible area contributing to surface runoff (dimensionless)	CAM	Surface runoff	10%

^a The six model parameters are spatially distributed, and thus their calibrated values have a range.

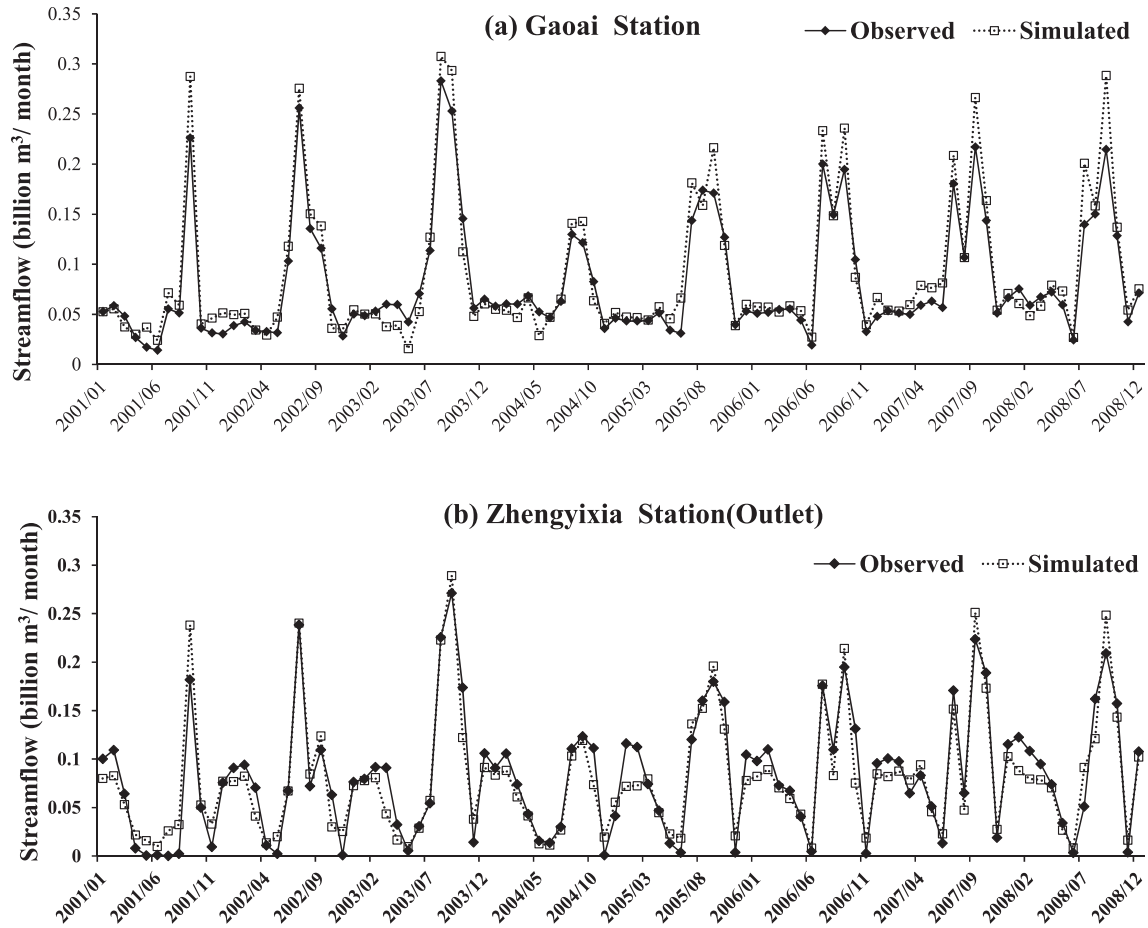


Fig. 3. Comparison of simulated and observed monthly streamflow at (a) the Gaoai station; and (b) the Zhengyixia station.

many wells, the calibrated model can still capture the main temporal trend, as demonstrated by Fig. 5. The five selected wells are located in places where the groundwater fluctuation is controlled by the SW-GW interaction and less impacted by the pumping.

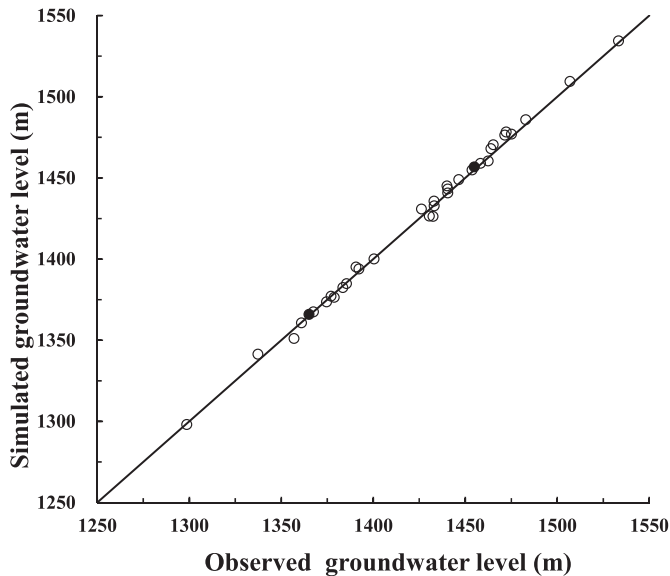


Fig. 4. Comparison of the observed and simulated groundwater levels averaged for the period 2001–2004. Each circle represents one of the 35 observation wells.

Some problems with the calibration were also observed, which could be mainly due to data imperfections. First, the logNSE at the Zhengyixia station is relatively small, because the near-zero flow during April to June was not well simulated (Fig. 3). Since the flow at the upstream Gaoai station during the same period was significant and the Heihe River between Gaoai and Zhengyixia is not a losing segment, the near-zero flow has to be caused by the substantial water diversion for irrigation in this segment. It therefore suggests that the diversion data we collected and input into the model may underestimate the actual amount during that period. Second, the positive BIAS (i.e., 0.09) at the Gaoai station is relatively high, mainly because the peak flow was overestimated in most of the years (Fig. 3). It is known that the local precipitation contributes a limited amount of water to the streamflow at Gaoai, and the peak flow at that point largely reflects the peak flow out of Yingluoxia (around 65 km upstream of Gaoai) which has been well gaged. On the other hand, the stream leakage in the segment between Yingluoxia and Gaoai has already been tuned to an appropriate level, referring to field measurements and isotope experiments (Wu et al., 2010). Thus, the systematic overestimation is most likely caused by the inaccurate (underestimated) diversion data of this segment. Third, the smaller NSE values for the daily streamflow simulation may be due to the inaccuracy of daily diversion estimates that were downscaled from the monthly diversion data.

As discussed in Bennett et al. (2013), a number of metrics, besides NSE, logNSE and BIAS, could be considered to quantitatively evaluate the model performance, and the calibration procedure in this study is not a rigorous method for the evaluation. Nevertheless,

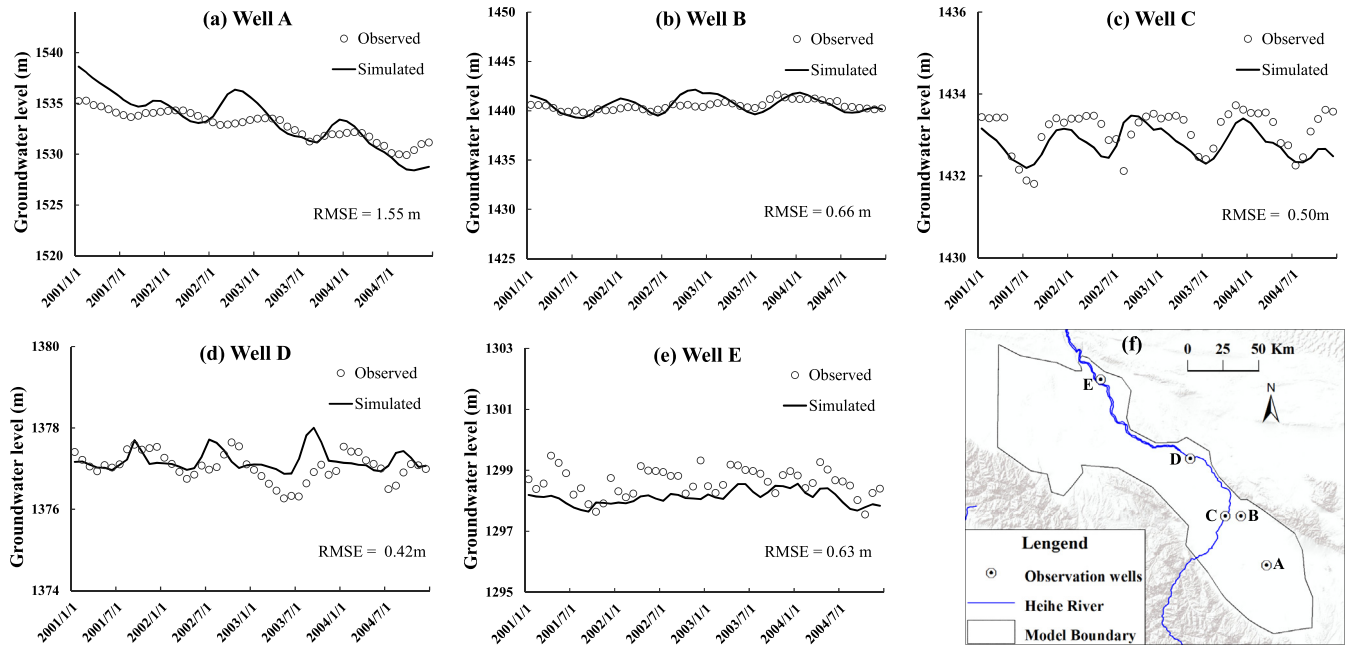


Fig. 5. Temporal variation of groundwater level at five selected observation wells. (a)–(e) comparison between the model simulation and observations; and (f) the locations of the wells.

our confidence on the model performance is based on the following two facts. First of all, both SWMM and GSFLOW (MODFLOW + PRMS) are well established models, and their theoretical basis and numerical performance have been examined in many studies. This study was aimed to evaluate the appropriateness and benefit of the model coupling, rather than the two individual models. Based on the metrics used in the calibration, we can conclude that the simulation capacity of both SWMM and GSFLOW has been well inherited, and the model coupling is technically sound. On the other hand, the hydrographs at the two stations (Fig. 3) would be greatly impacted by the diversion practice, as implied by the diversion points shown in Fig. 2, and the groundwater dynamics at the 35 observations wells (Fig. 2) could be highly sensitive to the substantial pumping. Thus, as manifested in our manual calibration procedure, it would be impossible to achieve the satisfactory goodness-of-fit if the effect of diversion and pumping were not properly taken into account. This embodies the value of the model integration attempted by this study. Secondly, in addition to the quantitative evaluation using the metrics, qualitative assessments were also conducted by eliciting the expert

opinion from China Geological Survey and the local water resources authorities. It was found that our modeling results of the regional water budget (see Section 4.3) and in-stream SW-GW interaction (see Section 4.4) are consistent with their field data-based understandings. This type of qualitative assessment can be essential in highly complex or data-poor situations (Bennett et al., 2013), like this study case.

4.2. Sensitivity results

Table 4 summarizes the sensitivity results (i.e., the elasticities). The abbreviations have been explained in Section 3.4. All the model outputs in the table are with regard to the annual average condition over the simulation period of 2001–2008. The bold numbers in the table are elasticities whose absolute values are over 0.1. Abundant information can be drawn on the regional water cycle, as well as on the modeling uncertainty, as discussed below.

ET and infiltration (IFL) are most sensitive to Precipitation (PCP), which reflects the water-limited condition of this semi-arid region. The sensitivity to PCP also suggests that more and better

Table 4 Sensitivity of 13 model outputs to 9 key input variables (the bold numbers are elasticities whose absolute values are over 0.1).

Model output	ID	Input variable								
		PCP	GWB	HK	VK	RVK	SY	SMM	SRM	CAM
Evapotranspiration	ET	0.30	0.04	0.00	0.00	0.01	0.00	-0.04	0.03	-0.04
Soil moisture	SM	0.12	0.10	-0.02	-0.01	0.00	0.01	1.27	-0.49	-0.02
Infiltration	IFL	0.31	0.01	0.00	0.00	0.01	0.00	-0.05	0.01	-0.05
Streamflow (outlet)	R	0.29	0.29	0.03	0.00	0.01	0.05	0.12	-0.07	0.13
GW level	H	0.00	0.03	-0.02	0.00	0.00	0.00	0.00	0.00	0.00
UZF recharge	UR	0.08	0.19	0.14	0.05	0.01	0.05	-0.07	-0.30	-0.05
GW exfiltration	GE	0.00	0.92	0.15	0.02	0.03	0.08	0.12	-0.20	-0.01
Stream to aquifer	R2G	0.07	-0.02	0.05	0.03	0.66	-0.03	0.04	0.00	0.00
Aquifer to stream	G2R	0.02	0.26	0.06	0.02	0.56	0.06	-0.01	0.00	0.00
SW to GW	S2G	0.07	0.02	0.07	0.03	0.54	-0.01	0.02	-0.05	-0.01
GW to SW	G2S	0.01	0.39	0.08	0.02	0.44	0.07	0.01	-0.04	-0.01
GW storage change	ΔS_{gw}	-0.64	-0.12	0.29	-0.10	0.74	0.58	-0.01	0.04	0.00
Total storage change	ΔS_{total}	-0.43	-0.10	0.16	-0.02	0.43	0.25	0.01	0.06	0.04

precipitation data are desired to improve the estimation of ET and IFL, since only six meteorological stations (see Fig. 2) are currently available for interpolating the distribution of precipitation.

For those SW-GW exchange fluxes (i.e., from UR to G2S in Table 4), GW lateral inflow (GWB) and hydraulic conductivity of streambed (RVK) appear to be the most influential factors, which indicates that the GW-SW exchange mostly occurs in the river and largely depends on the subsurface boundary inflow from the upstream. As GWB and RVK are highly uncertain input and parameter, respectively, in the modeling, hydrogeological surveys are desired to achieve more accurate data for reducing the modeling uncertainty.

Soil moisture (SM) is most sensitive to the two soil parameters soil's maximum available capillary water-holding capacity (SMM) and maximum depth where ET can occur (SRM). As PCP and GWB represent two important water inputs to the system, they also have a notable impact on SM. For streamflow at the outlet (R), besides PCP and GWB, SMM and maximum possible area contributing to surface runoff (CAM) were found to be important as well. These sensitivity results were well expected, given the hydrological meanings of the input variables (refer to Table 2). GW level (H), however, appears to be insensitive to all the input variables. This is not because H does not respond to them, but because the elasticity is not an appropriate sensitivity measure for H. H is defined based on elevation which is above 1000 m in this area. Thus, the variation of H (usually several meters) is order of magnitude lower than the elevation, which results in the small elasticity values.

On the other hand, the impact of the input variables on the groundwater system is well demonstrated by the sensitivity of GW storage change (ΔS_{gw}). Besides PCP, GWB and RVK, horizontal hydraulic conductivity (HK) and specific yield (SY) are two additional influential parameters for ΔS_{gw} , since they determine how fast and how much water could be released from the aquifer. Total storage change (ΔS_{total}) exhibits a similar sensitivity pattern as ΔS_{gw} , which reflects the modeling result that ΔS_{gw} is a major component of ΔS_{total} (see Section 4.3 for more details).

Overall, the sensitivity analysis demonstrated that the integrated modeling is valuable for understanding the water cycle in a large basin with complicated SW-GW interaction.

4.3. Regional water budget

Figs. 3–5 suggest that the GSFLOW-SWMM model has been adequately calibrated to simulate the general behavior of the SW-GW system in ZB. The simulated annual water budget (averaged

over 2001–2008) is illustrated by Fig. 6. It can be seen that the surface water inflow from the upper HRB is the top input (around 58%) to the system, followed by local precipitation and groundwater boundary inflow. Most of the total water input (around 77%) is eventually turned into ET, and the outflow from Zhengyixia accounts for about 26% of the total input. The lateral groundwater outflow is zero, which is the model assumption.

The SW-GW exchanges in both directions are significant with magnitudes comparable to those of surface water outflow and local precipitation. But the net exchange, from GW to SW, is relatively small (0.134 billion m^3 /year) and much less than the pumped groundwater. The total groundwater recharge (S2G) consists of two parts, one from streams (R2G, equal to 0.813 billion m^3 /year) and the other from infiltration water (UR, equal to 0.155 billion m^3 /year). According to the modeling, around 53% of UR (0.082 billion m^3 /year) is on irrigated lands. On the other hand, the total groundwater discharge (G2S) consists of the discharge to stream (G2R, equal to 0.889 billion m^3 /year) and exfiltration to land surface (GE, equal to 0.213 billion m^3 /year).

The negative ΔS_{total} is mainly due to the depletion of the groundwater storage (-0.08 billion m^3 /year) and the drying of the unsaturated zone (-0.066 billion m^3 /year), which implies that the current water use may not be sustainable in the long term and proper management measures are desired. Note that the surface water diversion is 1.728 billion m^3 /year on average, much larger than the difference between SW_{in} and SW_{out} (1.235 billion m^3 /year), which implies that a significant amount of the irrigation water returns to the stream in a short time period, either as surface runoff or groundwater flow. All the above results suggest that the SW-GW interaction plays a critical role in the hydrologic cycle.

4.4. SW-GW interaction

The leakage from the main stream of the Heihe River is 0.53 billion m^3 /year (about 65% of R2G), and the groundwater discharge to the main stream is 0.70 billion m^3 /year (about 79% of G2R). Apparently, the SW-GW exchanges mostly occur in the main stream. Fig. 7 illustrates the simulated monthly exchange rates (averaged over 2001–2008) in the main stream. Positive values indicate river leakage to aquifer, and negative values indicate groundwater discharge to river. The data of monthly inflow from Yingluoxia and water diversion are also plotted for comparison. The leakage has a more notable seasonal variation than the discharge, and high net exchange rates occur in the flood season (July to September).

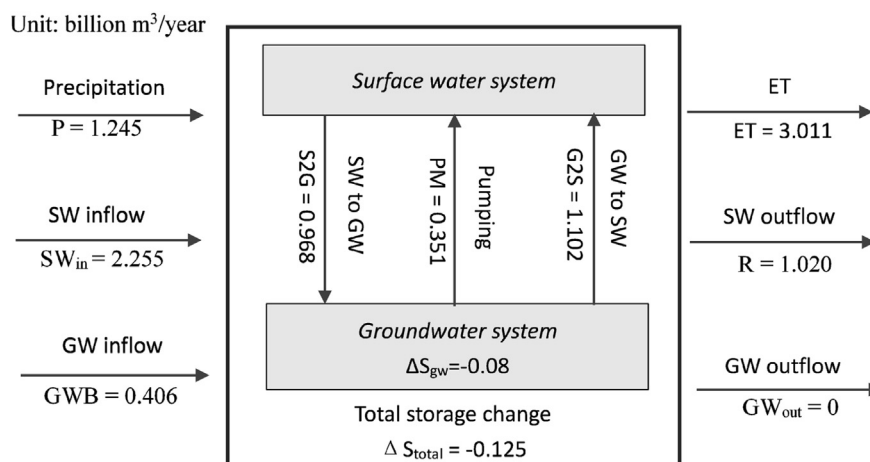


Fig. 6. Average annual water budget simulated by the GSFLOW-SWMM model.

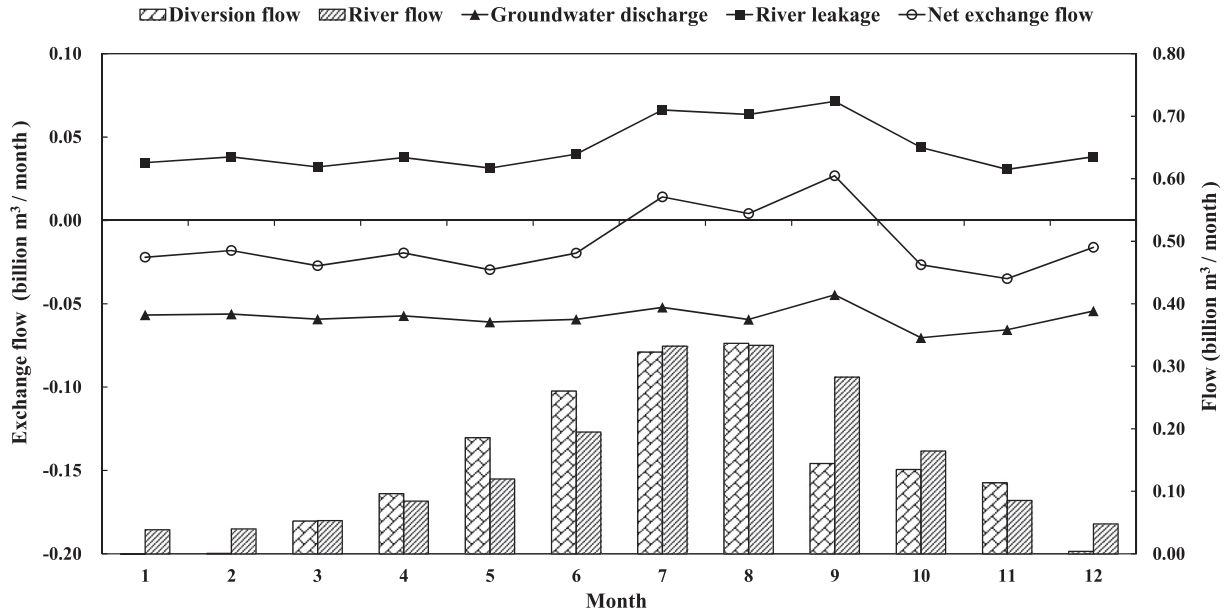


Fig. 7. Seasonal variation of the surface water-groundwater interaction in the main stream of the Heihe River, averaged for 2001–2008.

Generally speaking, larger streamflow would result in an elevated surface water head and therefore more river leakage and less groundwater discharge. But this general trend is complicated by the diversion practice in this area. For example, November has a higher flow rate than December to March, but its diversion rate is also significantly higher, which explains why November has the minimal river leakage in a year. The difference between April and May can be similarly explained. Fig. 8 illustrates the dependence of both the leakage and discharge on the flow at the Yingluoxia station, based on the model simulation. While the leakage maintains an expected positive correlation with the flow, no significant correlation has been observed for the groundwater discharge.

Fig. 9 further demonstrates the spatial patterns of the SW-GW exchange flux (i.e., volume of water per unit area of streambed per unit time) along the main stream. Three segments with distinct exchange patterns are clearly identified (Fig. 9a). The upper segment, extending from Yingluoxia to a key point named “312 Bridge”, is a “losing segment”. This 35-km segment has a steep streambed slope of around 0.01, and the depth (from the streambed) to water table varies from approximately 170 m–0 m. In this segment, the flow is disconnected with the aquifer until it approaches the 312 Bridge, and the net exchange from SW to GW is 0.53 billion m³/year. After the 312 bridge, the streamflow is hydraulically connected with the aquifer. From the 312 Bridge to the

point of Pingchuan is a “gaining segment”. The streambed slope decreases to less than 0.001 in this 65-km segment. The head difference is negative (i.e. groundwater level is higher than the river water stage) in this segment (see Fig. 9b), and the net exchange rate (from GW to SW) is –0.7 billion m³/year. From Pingchuan down, the head difference is small (see Fig. 9c), and the river leakage and groundwater discharge are roughly equal, with a net exchange of 0.03 billion m³/year. This segment is therefore referred as a “balanced segment”. The spatial patterns illustrated by Fig. 9 agree well with the field observations (Hu et al., 2012).

Fig. 9a also shows the seasonal variation of the SW-GW exchange by comparing three conditions including annual average, July (with the highest inflow) and January (with the lowest inflow). The seasonal variation is significant only in the losing segment. In July, the net exchange rate has an abrupt decline at a point 10 km away from Yingluoxia, which is in fact caused by the substantial water diversion at this point.

Interestingly, Figs. 7 and 9 imply that the local aquifers act as huge groundwater reservoirs. In time, the groundwater storage is replenished in wet seasons and releases water back to the river in dry seasons. In space, the storage is replenished in the upper segment and returns water back in the middle segment. Such a system behavior provides a possibility to better allocate the limited water resources both in time and space by implementing artificial

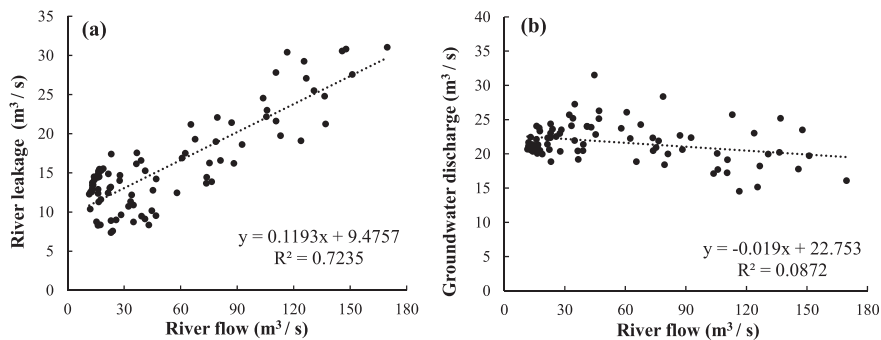


Fig. 8. Correlations between the streamflow at the Yingluoxia station and (a) the river leakage; and (b) the groundwater discharge.

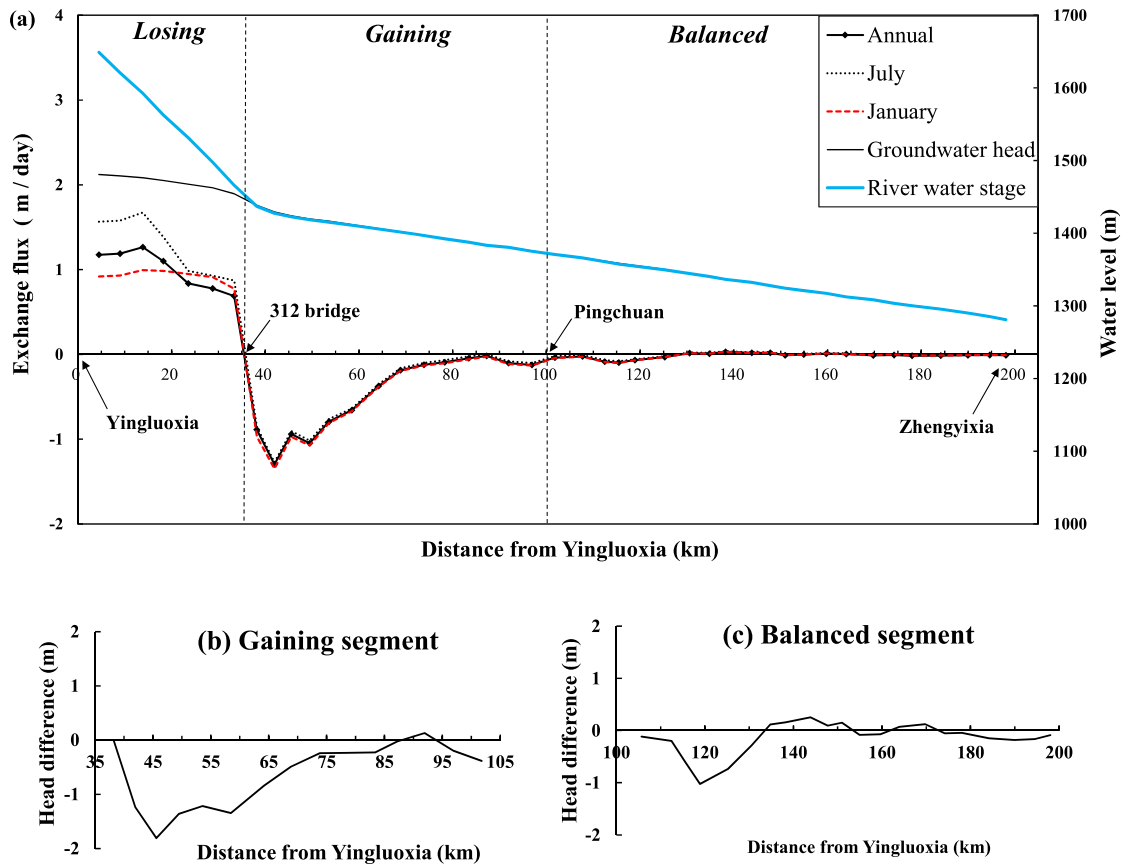


Fig. 9. Spatial and temporal variation of the surface water-groundwater interaction along the main stream of the Heihe River. (a) The complete profiles of exchange flux and head difference; (b) the profile of head difference in the gaining segment; and (c) the profile of head difference in the balanced segment.

recharge (Giao et al., 1998; Shah, 2014) instead of building large reservoirs which may introduce many ecological problems.

4.5. Scenario analysis results

Fig. 10 compares the five water use scenarios (Table 1). Fig. 10a shows that, in the study area, reducing diversion in combination with increasing pumping would lead to higher surface outflow and faster storage depletion, which can be explained as follows. Diversion reduction would increase the river stage and consequently enhance the stream recharge to groundwater and inhibit the groundwater discharge to stream. Therefore, the groundwater would be replenished by the diversion reduction. However, according to the model, if a same amount of groundwater is pumped to substitute the diversion, the pumpage would significantly exceed the replenishment induced by the reduction of diversion. The change of ET is small since the total irrigation water remains the same. Fig. 10b provides more details on the change of different storage components. It is clear that the major difference in the total storage change is due to the difference in the change of groundwater (i.e., saturated zone) storage.

Fig. 10c illustrates how the SW-GW interaction would respond. It shows that substitution of SW diversion by GW pumping would decrease the groundwater discharge but increase the groundwater recharge, and the former is more sensitive to the scenario change. Thus, the net flux from GW to SW would be reduced due to the water source substitution. The decline of groundwater discharge may lead to two ecological problems. First, the base-flow would be reduced, which may have a negative impact on the river aquatic

ecosystem (Hancock et al., 2005). Second, wetlands in ZB would be jeopardized. There are many wetlands in the study area which are sustained by springs (i.e., groundwater exfiltration). These wetlands are critical to the sustainability of the desert-oasis ecosystem in ZB.

Overall, Fig. 10 implies that, if the irrigation demand in ZB keeps increasing, implementation of the current water allocation plan would accelerate the depletion of the local aquifers, which may introduce ecological problems to the middle HRB. Thus, if the water allocation is not accompanied by an appropriate regulation on the groundwater pumping in ZB, which is the current situation, there exists a tradeoff between the recovery of the ecosystem in the lower HRB and the health of the ecosystem in the middle HRB. It is imperative to develop a holistic solution to reduce the irrigation water consumption by improving the water resources productivity in this area.

5. Conclusions

In this study, GSFLOW and the hydraulic engine of SWMM were successfully coupled, and additional improvements were made. The new model, referred to as GSFLOW-SWMM, can effectively address a complicated irrigation system with both surface water diversion and groundwater pumping. The case study in the Zhangye Basin demonstrated the applicability of the model for large basins, as well as its strength in providing a holistic view of the water cycle, characterizing the SW-GW interaction with sufficient spatial and temporal details, and supporting real-world management decisions.

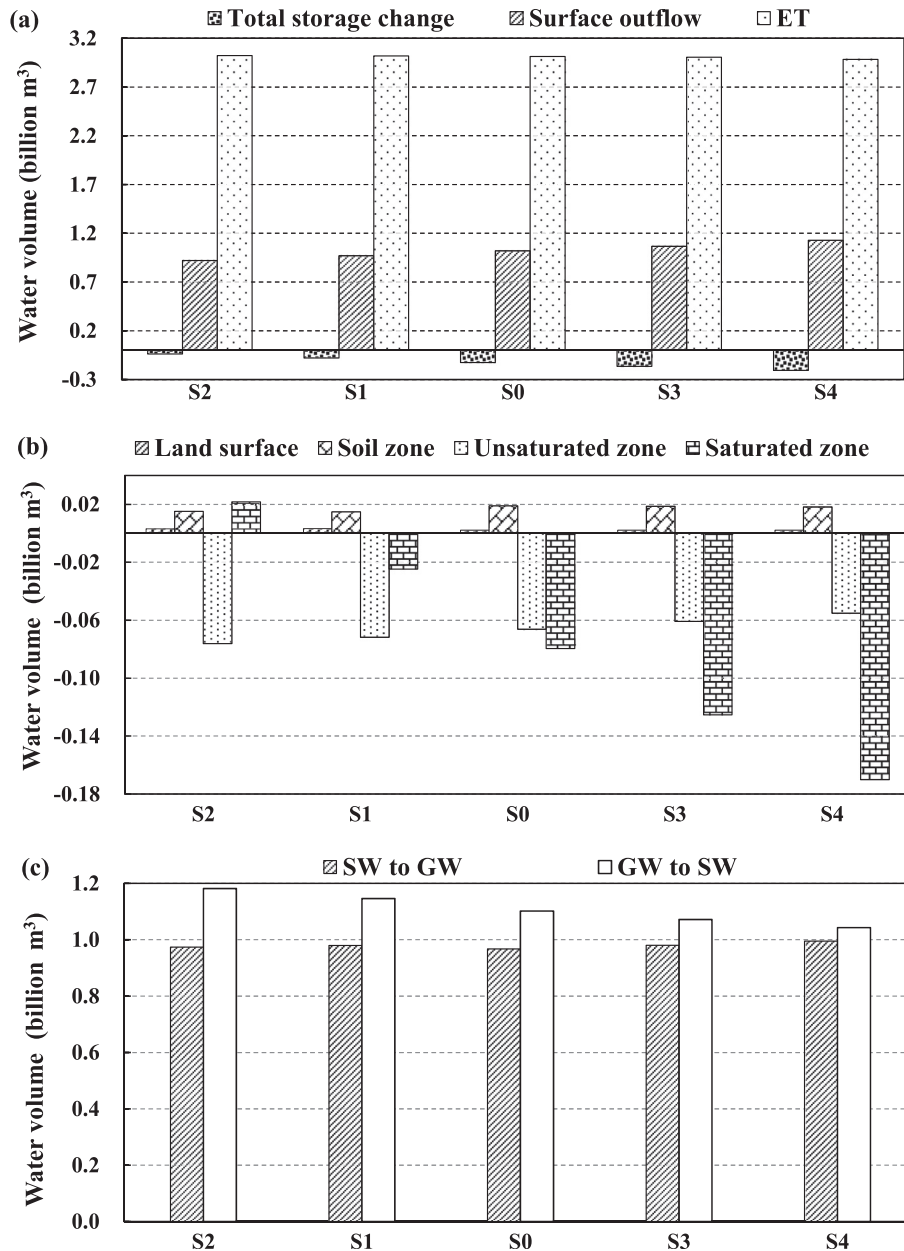


Fig. 10. Water balance in five simulated management scenarios (S0 is the baseline scenario). (a) Outflows and total storage changes; (b) storage changes; and (c) SW-GW exchanges.

Major findings of the case study include the following. First, the SW-GW interaction in the study area is significant and mainly occurs in the main stream of Heihe River. Second, the in-stream SW-GW exchange has notable spatial and temporal variations, and is impacted by both surface water diversion and groundwater pumping. Third, although the existing water allocation plan has been effective to guarantee the environmental flow to the lower HRB, it has encouraged the relatively unregulated groundwater pumping in this area. In the long-run, the recovery of the ecosystem in the lower HRB may be at the cost of the health of the ecosystem in the middle HRB. A holistic water management solution is imperatively needed to achieve the sustainability of the eco-hydrological system in HRB.

It is worth pointing out that some limitations of the coupled model remain and deserve further studies. First, the model setup, especially for the GSFLOW part, has not been streamlined and automated, and external tools and substantial manual operations are needed. Software specifically designed for the model setup is

highly desired. Second, water diversion and pumping data are critical model inputs, but are often hard to achieve. Even if available, they usually have low spatial and temporal resolutions and involve significant uncertainty. Future studies may consider developing a module to simulate demand-based diversion and pumping rates in space and time. Third, SWMM has a well-developed water quality module, which has not been incorporated into GSFLOW-SWMM yet. Since water quality issues (e.g., salinity, nutrients, etc.) are interrelated with water resources issues in arid and semi-arid regions with intensive agriculture, it would be of great research interests to extend GSFLOW-SWMM to an integrated water quality model.

Acknowledgments

This work was supported by the National Natural Science Foundation of China (NSFC) (No. 91125021, No. 91225301 and No.

41371473). The data set was provided by Cold and Arid Regions Science Data Center in Lanzhou, China (<http://westdc.westgis.ac.cn>). We also thank the three anonymous reviewers for their insightful comments and suggestions.

References

- Adeboye, O.B., Osunbitan, J.A., Adekalu, K.O., Okunade, D.A., 2009. Evaluation of FAO-56 Penman–Monteith and temperature based models in estimating reference evapotranspiration using complete and limited data, application to Nigeria. *Agric. Eng. Int. CIGR J.* 11, 1–25.
- Allen, R.G., Pereira, L.S., Raes, D., Smith, M., 1998. *Crop Evapotranspiration—Guidelines for Computing Crop Water Requirements—FAO Irrigation and Drainage Paper 56*. Food and Agriculture Organization of the United Nations, Rome, Italy.
- Arnold, J.G., Srinivasan, R., Muttiah, R.S., Williams, J.R., 1998. Large area hydrologic modeling and assessment part I: model development. *JAWRA J. Am. Water Resour. Assoc.* 34 (1), 73–89.
- Barlow, P.M., DeSimone, L.A., Moench, A.F., 2000. Aquifer response to stream–stage and recharge variations. II. Convolution method and applications. *J. Hydrol.* 230 (3–4), 211–229.
- Bennett, N.D., Croke, B.F.W., Guariso, G., Guillaume, J.H.A., Hamilton, S.H., Jakeman, A.J., Marsili-Libelli, S., Newham, L.T.H., Norton, J.P., Perrin, C., Pierce, S.A., Robson, B., Seppelt, R., Voinov, A.A., Fath, B.D., Andreassian, V., 2013. Characterising performance of environmental models. *Environ. Model. Softw.* 40, 1–20.
- Borah, D.K., Bera, M., 2003. Watershed–scale hydrologic and nonpoint–source pollution models: review of mathematical bases. *Trans. ASAE* 46 (6), 1553–1566.
- Brunner, P., Simmons, C.T., 2012. HydroGeoSphere: a fully integrated, physically based hydrological model. *Ground Water* 50 (2), 170–176.
- Chen, Z., Nie, Z., Zhang, G., Wan, L., Shen, J., 2006. Environmental isotopic study on the recharge and residence time of groundwater in the Heihe River Basin, northwestern China. *Hydrogeol. J.* 14 (8), 1635–1651.
- Cheng, G.D., Xiao, H.L., Zhao, W.Z., Feng, Q., Xu, Z.M., Li, X., 2009. *Water-ecological-economic System Integrated Management Research on Heihe River Basin (in Chinese)*. Science Press, Beijing.
- Demetriou, C., Punthakey, J.F., 1998. Evaluating sustainable groundwater management options using the MIKE SHE integrated hydrogeological modelling package. *Environ. Model. Softw.* 14 (2–3), 129–140.
- Feng, Q., Cheng, G.D., 2001. Towards sustainable development of the environmentally degraded River Heihe basin, China. *HydroSci.* 46 (5), 647–658.
- Fisher, J.B., Whittaker, R.J., Malhi, Y., 2011. ET come home: potential evapotranspiration in geographical ecology. *Glob. Ecol. Biogeogr.* 20 (1), 1–18.
- Giao, P.H., Phien–Wej, N., Honjo, Y., 1998. FEM quasi-3D modelling of responses to artificial recharge in the Bangkok multiaquifer system. *Environ. Model. Softw.* 14 (2–3), 141–151.
- Gilfedder, M., Rassam, D.W., Stenson, M.P., Jolly, I.D., Walker, G.R., Littleboy, M., 2012. Incorporating land-use changes and surface–groundwater interactions in a simple catchment water yield model. *Environ. Model. Softw.* 38, 62–73.
- Gironás, J., Roesner, L.A., Rossman, L.A., Davis, J., 2010. A new applications manual for the Storm Water Management Model (SWMM). *Environ. Model. Softw.* 25 (6), 813–814.
- Graham, D.N., Butts, M.B., 2005. Flexible, integrated watershed modelling with MIKE SHE. In: V.P., S., D.K., F. (Eds.), *Watershed Models*. CRC Press, pp. 245–272.
- Guo, Q., Feng, Q., Li, J., 2009. Environmental changes after ecological water conveyance in the lower reaches of Heihe River, northwest China. *Environ. Geol.* 58 (7), 1387–1396.
- Hancock, P., Boulton, A., Humphreys, W., 2005. Aquifers and hyporheic zones: towards an ecological understanding of groundwater. *Hydrogeol. J.* 13 (1), 98–111.
- Harbaugh, A.W., 2005. MODFLOW–2005. The U.S. Geological Survey modular groundwater model—the ground-water flow process. USGS Techniques and Methods: 6–A16. Available at: <http://pubs.usgs.gov/tm/2005/tm6A16/PDF.htm> (accessed 07.03.14.).
- Hu, L., Chen, C., Jiao, J.J., Wang, Z., 2007. Simulated groundwater interaction with rivers and springs in the Heihe river basin. *Hydrol. Process.* 21 (20), 2794–2806.
- Hu, X., Xiao, H., Lan, Y., 2012. Experimental study of calculating method of river Seepage in middle and upper reaches of the heihe river (in chinese). *J. Glaciol. Geocryol.* 2, 460–468.
- Huntington, J.L., Niswonger, R.G., 2012. Role of surface–water and groundwater interactions on projected summertime streamflow in snow dominated regions: an integrated modeling approach. *Water Resour. Res.* 48 (11), W11524.
- Leavesley, G.H., Lichty, R.W., Troutman, B.M., Saindon, L.G., 1983. *Precipitation–runoff Modeling System; User’s Manual* USGS Water–resources Investigations Report. USGS Water–Resources Investigations Report: 83–4238, 206pp. Available at: <http://pubs.usgs.gov/wri/1983/4238/report.pdf> (accessed 07.03.14.).
- Li, X., Cheng, G., Liu, S., Xiao, Q., Ma, M., Jin, R., Che, T., Liu, Q., Wang, W., Qi, Y., Wen, J., Li, H., Zhu, G., Guo, J., Ran, Y., Wang, S., Zhu, Z., Zhou, J., Hu, X., Xu, Z., 2013. Heihe Watershed Allied Telemetry Experimental Research (HiWATER): scientific objectives and experimental design. *Bull. Am. Meteorol. Soc.* 94 (8), 1145–1160.
- Li, X.M., Lu, L., Yang, W.F., Cheng, G.D., 2012. Estimation of evapotranspiration in an arid region by remote sensing—A case study in the middle reaches of the Heihe River Basin. *Int. J. Appl. Earth Obs. Geoinform.* 17, 85–93.
- Li, Z., Shao, Q., Xu, Z., Cai, X., 2010. Analysis of parameter uncertainty in semi-distributed hydrological models using bootstrap method: a case study of SWAT model applied to Yingluoxia watershed in northwest China. *J. Hydrol.* 385 (1–4), 76–83.
- Liu, W., Cao, S., Xi, H., Feng, Q., 2010. Land use history and status of land desertification in the Heihe River basin. *Nat. Hazards* 53 (2), 273–290.
- Luo, F., Qi, S.Z., Xiao, H.L., 2005. Landscape change and sandy desertification in arid areas: a case study in the Zhangye Region of Gansu Province, China. *Environ. Geol.* 49, 90–97.
- Markstrom, S.L., 2012. *Integrated Watershed–scale Response to Climate Change for Selected Basins across the United States*. U.S. Geological Survey Scientific Investigations Report 2011–5077, 143pp. Available at: http://pubs.usgs.gov/sir/2011/5077/SIR11-5077_508.pdf (accessed 07.03.14.).
- Markstrom, S.L., Niswonger, R.G., Regan, R.S., Prudic, D.E., Barlow, P.M., 2008. GSFLOW—Coupled Ground–water and Surface–water FLOW Model Based on the Integration of the Precipitation–runoff Modeling System (PRMS) and the Modular Ground–water Flow Model (MODFLOW–2005). U.S. Geological Survey Techniques and Methods 6–D1, 240pp. Available at: <http://pubs.usgs.gov/tm/tm6d1/pdf/tm6d1.pdf> (accessed 07.03.14.).
- McCallum, A.M., Andersen, M.S., Giambastiani, B.M.S., Kelly, B.F.J., Ian Acworth, R., 2013. River–aquifer interactions in a semi–arid environment stressed by groundwater abstraction. *Hydrol. Process.* 27 (7), 1072–1085.
- Nalder, I.A., Wein, R.W., 1998. Spatial interpolation of climatic Normals: test of a new method in the Canadian boreal forest. *Agric. For. Meteorol.* 92 (4), 211–225.
- Nash, J.E., Sutcliffe, J.V., 1970. River flow forecasting through conceptual models part I — a discussion of principles. *J. Hydrol.* 10 (3), 282–290.
- Niswonger, R.G., Prudic, D.E., 2005. Documentation of the Streamflow–routing (SFR2) Package to Include Unsaturated Flow beneath Streams—a Modification to SFR1. U.S. Geological Survey Techniques and Methods 6–A13, 50 pp. Available at: <http://pubs.usgs.gov/tm/2006/tm6A13/pdf/tm6A13.pdf> (accessed 07.03.14.).
- Niswonger, R.G., Prudic, D.E., Fogg, G.E., Stonestrom, D.A., Buckland, E.M., 2008. Method for estimating spatially variable seepage loss and hydraulic conductivity in intermittent and ephemeral streams. *Water Resour. Res.* 44 (5), W05418.
- Niswonger, R.G., Prudic, D.E., Regan, R.S., 2006. Documentation of the Unsaturated–zone Flow (UZFI) Package for Modeling Unsaturated Flow between the Land Surface and the Water Table with MODFLOW–2005. U.S. Geological Survey Techniques and Methods, 6–A19, 62 pp. Available at: <http://pubs.usgs.gov/tm/2006/tm6A19/pdf/tm6A19.pdf> (accessed 07.03.14.).
- Pérez, A.J., Abrahão, R., Causapé, J., Cirpka, O.A., Bürger, C.M., 2011. Simulating the transition of a semi–arid rainfed catchment towards irrigation agriculture. *J. Hydrol.* 409 (3–4), 663–681.
- Panday, S., Huyakorn, P.S., 2004. A fully coupled physically–based spatially–distributed model for evaluating surface/subsurface flow. *Adv. Water Resour.* 27 (4), 361–382.
- Peterson, E.W., Wicks, C.M., 2006. Assessing the importance of conduit geometry and physical parameters in karst systems using the storm water management model (SWMM). *J. Hydrol.* 329 (1–2), 294–305.
- Rassam, D.W., 2011. A conceptual framework for incorporating surface–groundwater interactions into a river operation–planning model. *Environ. Model. Softw.* 26 (12), 1554–1567.
- Rassam, D.W., Peeters, L., Pickett, T., Jolly, I., Holz, L., 2013. Accounting for surface–groundwater interactions and their uncertainty in river and groundwater models: a case study in the Namoi River, Australia. *Environ. Model. Softw.* 50 (0), 108–119.
- Rossman, L.A., 2009. *Storm Water Management Model User’s Manual Version 5.0*. U.S. Environmental Protection Agency, EPA/600/R-05/040. Available at: <http://nepis.epa.gov/Adobe/PDF/P10011XQ.pdf> (accessed 07.03.14.).
- Rodriguez, L.B., Cello, P.A., Vionnet, C.A., Goodrich, D., 2008. Fully conservative coupling of HEC–RAS with MODFLOW to simulate stream–aquifer interactions in a drainage basin. *J. Hydrol.* 353 (1–2), 129–142.
- Shah, T., 2014. Towards a Managed Aquifer Recharge strategy for Gujarat, India: an economist’s dialogue with hydro–geologists. *J. Hydrol.* 518, 94–107.
- Shrestha, N.K., Leta, O.T., De Fraine, B., van Griensven, A., Bauwens, W., 2013. OpenMI–based integrated sediment transport modelling of the river Zenne, Belgium. *Environ. Model. Softw.* 47 (0), 193–206.
- Siebert, S., Burke, J., Faures, J.M., Frenken, K., Hoogeveen, J., Döll, P., Portmann, F.T., 2010. Groundwater use for irrigation — a global inventory. *Hydrol. Earth Syst. Sci. Discuss.* 7 (3), 3977–4021.
- Singh, V.P., 2001. Kinematic wave modelling in water resources: a historical perspective. *Hydrol. Process.* 15 (4), 671–706.
- Sophocleous, M., 2002. Interactions between groundwater and surface water: the state of the science. *Hydrogeol. J.* 10 (1), 52–67.
- Sophocleous, M.A., Koelliker, J.K., Govindaraju, R.S., Birdie, T., Ramireddygar, S.R., Perkins, S.P., 1999. Integrated numerical modeling for basin–wide water management: the case of the Rattlesnake Creek basin in south–central Kansas. *J. Hydrol.* 214 (1–4), 179–196.
- Therrien, R., McLaren, R.G., Sudicky, E.A., Panday, S.M., 2010. *HydroGeoSphere A Three–dimensional Numerical Model Describing Fully–integrated Subsurface and Surface Flow and Solute Transport*. Technical report.
- Valerio, A., Rajaram, H., Zagana, E., 2010. Incorporating Groundwater–Surface water interaction into river management models. *Ground Water* 48 (5), 661–673.

- VanderKwaak, J.E., Loague, K., 2001. Hydrologic–Response simulations for the R–5 catchment with a comprehensive physics–based model. *Water Resour. Res.* 37 (4), 999–1013.
- Vieira, J.H.D., 1983. Conditions governing the use of approximations for the Saint–Venant equations for shallow surface water flow. *J. Hydrol.* 60 (1–4), 43–58.
- Wang, X.S., Ma, M.G., Li, X., Zhao, J., Dong, P., Zhou, J., 2010. Groundwater response to leakage of surface water through a thick vadose zone in the middle reaches area of Heihe River Basin, in China. *Hydrol. Earth Syst. Sci.* 14 (4), 639–650.
- Welsh, W.D., Vaze, J., Dutta, D., Rassam, D., Rahman, J.M., Jolly, I.D., Wallbrink, P., Podger, G.M., Bethune, M., Hardy, M.J., Teng, J., Lerat, J., 2013. An integrated modelling framework for regulated river systems. *Environ. Model. Softw.* 39 (0), 81–102.
- Wen, X.H., Wu, Y.Q., Lee, L.J.E., Su, J.P., Wu, J., 2007. Groundwater flow modeling in the Zhangye Basin, northwestern China. *Environ. Geol.* 53 (1), 77–84.
- Werner, A.D., Gallagher, M.R., Weeks, S.W., 2006. Regional–scale, fully coupled modelling of stream–aquifer interaction in a tropical catchment. *J. Hydrol.* 328 (3–4), 497–510.
- Wu, Y.Q., Zhang, Y.H., Wen, X.H., Su, J.P., 2010. *Hydrologic Cycle and Water Resource Modeling for the Heihe River Basin in Northwestern China* (in Chinese). Science Press, Beijing.
- Zhang, G.H., Liu, S.Y., Xie, Y.B., 2004. *Water Cycle and Development of Groundwater in the Inland Heihe River Basin InWest–North China* (in Chinese). Geology Publication House, Beijing.